Strojniški vestnik - Journal of Mechanical Engineering 66(2020)2, 127-141

DOI:10.5545/sv-jme.2019.6320 Original Scientific Paper
Received for review: 2019-09-08
Received revised form: 2019-11-28
Accepted for publication: 2019-12-11

Mathematical Modelling Study of Hardox400 Steel Parts' Roughness and Hardness, Cut with CO_2 Laser

Mihaela Mileșan[1] – Constantin Cristinel Gîrdu[1] – Liviu Cîrtînă[2] – Constanța Rădulescu[2]

[1] Transylvania University of Brașov, Faculty of Technological Engineering and Industrial Management, Romania
[2] Constantin Brâncuși University, Romania

This study supports the research in the field of laser cutting of steel sheets HARDOX400 (H400), a less well-known and analysed material. An H400 sheet with a thickness of 10 mm was used; a cutting plan was prepared according to Taguchi's method; the input parameters (laser power, assistant gas pressure and cutting speed) were varied according to a specific rule, producing nine pieces. The initial factorial experiment was replicated four times under the same conditions as the initial one. The values for the cutting width between the piece and the plate, the hardness, and the roughness of the 45 resulting pieces were measured. The results were interpreted for each measured parameter, and by using design of experiments (DOE) from the Statistics 7.0 software, we obtained the description of roughness (R_a) in terms of power and speed using Response Surface Method (RSM) for prediction and correlation formula.

Keywords: laser cutting, roughness, hardness, kerf, CO_2 laser, ANOVA analysis

Highlights

- *Indication of the mathematical expression of the roughness R_a from algebraic and differential points of view.*
- *Description of the cutting parameters of the CO_2 laser installation for cutting a Hardox400 plate according to a cutting plan, consisting of 45 pieces.*
- *The use of the response surface and the three dimensional (3D) graph to determine the roughness R_a depending on the input parameters, laser power, and cutting speed.*
- *Establishing the formula for correlating the roughness R_a according to the laser power and the cutting speed within the linear and quadric model, respectively the statistical calculation within the linear and quadratic interaction.*

0 INTRODUCTION

Adelmann and Hellman **[1]** explored current approaches, such as caustic laser beam and surrogate criterion, while operating the TRUMPF machine. After analysing every step of the process, they found that the focal position is an influential factor that ensures stability in production. They employed the fast laser cutting optimization algorithm (FALCOA) to speed up the laser cutting of Al thin sheets. The algorithm provided insights into the role of individual parameters (i.e., cutting speed, focal position, gas pressure, gas nozzle diameter) and their interactions, while also determining the variance of the cutting process, based on the examined parameters.

Lutey et al. **[2]** developed a technology for the long-pulse quasi-continuous-wave (quasi-CW) laser cutting of metals, executed with pulsed lasers, with pulse durations in the domain of milliseconds. These are obtained by tweaking the pump source to perform a continuous-wave operation (CW), which turns out to be a better solution for the processing of parts. The lowest roughness of the cut edge surface is obtained using oxygen gas, a process that takes place at the lowest average cutting power, resulting in the best cutting quality. The study recommends laser cutting of metals with oxygen-assisted quasi-CW long pulses, because it is a better solution in the manufacture of parts.

Ivarson et al. **[3]** observed that small variations in the chemical composition of different alloying elements (i.e., manganese, silicon, carbon) affect the laser-oxygen cutting process. The main factors that affect the process are the variation of the surface tension and the viscosity of the material, due to the exothermic reaction in the cutting area. Increasing the manganese content reduces the quality of the cut edge, i.e., a sharp edge, with adherent slag on the lower part of the cut. A higher silicon content leads to a higher quality of cut edges. Increasing the carbon content reduces the exothermic reaction when the manganese content is high, while also stabilising the laser cutting process. The paper quantifies the way in which the alloying elements affect the surface roughness and the appearance of slag on the lower edge of the cut due to the change in viscosity of molten steel, combined with changes resulting from the exothermic reaction.

Pocorni et al. **[4]** discuss stationary piercing and dynamic piercing, using high-speed imaging (HSI) to observe the behaviour of melt in the perforated slot.

*Corr. Author's Address: Transylvania University of Brașov, Bd. Eroilor no. 29, Brașov, Romania, mihaela.milesan@unitbv.ro

The HSI images show that, in the dynamic piercing, the circular rotation of the beam forces the melt to flow in the direction opposite the movement of the beam, while in the stationary piercing the melt spreads randomly in all directions, which creates defects (pores, slag, etc.) on the material.

Shulyateyev et al. [5] discovered some aspects that support the research of thick laser-cut sheets: the surface roughness increases with the thickness of the steel sheet, reducing the quality of the parts in various applications; the size and density of the striations increase with the thickness of the material sheet; emphasis is placed on the flow of the gas stream which is coaxial with the laser beam and which has a significant influence on the molten mass at the bottom, but also the dispersion of molten droplets on the walls, forming craters on the cut surfaces; Spreading hot liquid droplets from the molten mass and ejecting them from the channel using O_2 assistant gas results in a decreased roughness. Thicker laser-cut steel materials have rougher cut edges due to the burning reaction of iron with oxygen.

Thombansen et al. [6] showed that laser cutting in ramp-up management is facilitated by the control of focalization, because the laser-cutting machine reliably produces the components at the required quality and speed. The active control of the focal position ensures the stability of the focal position during processing, thus reducing the working time of the machine. Laser cutting is of high quality if the parameters of the cutting process (i.e., the focal position, the distance between the cutting nozzle and the workpiece, and the quality of the beam) are within the defined tolerances. The measurement solution of a surrogate criterion is translated by knowing the correlations and determining the focal position during the cutting processing ensured by the laser stability. The study indicates that laser-cut parts are of good quality if the cutting machinery is equipped with sensors that control the laser's focal position.

Zhang and Lei [7] present the Fuzzy Model used to predict the roughness of fibre or CO_2 laser cutting. The model is intelligently designed by exceeding the back-propagation (BP) neural network model. The algorithmic reasoning starts from elements of linear analysis, using input variables (e.g.. gas pressure, cutting speed, laser power, cutting width) and roughness, the output variable. Comparing the BP and ANFIS® models, which indicate the roughness prediction and the relative error, it appears that the data obtained with the ANFIS model are significantly less than that the from the BP model. The roughness is discussed according to the defined variables: laser power (P), cutting speed (v), the pressure of the assistant gas (p), cutting width (*Kerf*), using the response surfaces method. Therefore, the simultaneous influence of two physical quantities on the output parameter, roughness (R_a), can result from the mathematical relationships or measured, for comparison. In conclusion, better-polished surfaces have better roughness and, therefore, increased hardness. In other words, hardness varies directly with roughness.

Zhang et al. [8] developed research on the manufacturing of biomedical and aerospace industrial products made of stainless steel, AlSI 316L. This requires further processing of the parts to improve the finishing and dimensional accuracy, after the selective laser melting (SLM) technique. In the final SLM-induced stainless steel processing technique, the design of the tools that were coated with a nanotextured substrate was taken into account, leading to stabilization in terms of adhesion layer formation. By femtosecond ($1 \cdot 10^{-15}$ s) laser scanning, a periodic nano-processing structure was induced on the tungsten carbide cobalt WC-Co substrate instrument with different varied processing parameters. Then the TiAlN film was deposited on the surface of the nano-text substrate. A new instrument has been designed and manufactured by dry cutting (no cutting fluid) of the materials produced with SLM. Due to SLM, the obtained tools have a higher quality of materials. The adhesion of the TiAlN film coating is significantly increased by the periodic femtosecond laser induced structure on the WC-Co substrate, and the critical load of the TiAlN coatings increased from 57 M to 73 N.

Wang et al. [9] developed a laser-plating technology of the titanium alloy Ti-6Al-4V for the preparation of the coating layer and the milling experiment that takes place on the coating layer. It is found that if a laser-coated layer is processed, the milling force affects the roughness R_a and the surface topography. By adjusting the parameters milling speed v, feed per tooth fz, milling width $a(e)$, a small milling force and a good milling surface R_a result. The heat-affected zone (HAZ) width of the laser plating layer is 0.8 mm. Reducing the milling forces to obtain a good surface coating of the Ti-6Al-4V (TC4) layer shows a large v and fz and $a(e)$ to be selected. The study shows that the milling blade is substantially improved by laser plating of the Ti-6Al-4V alloy, resulting in the milling force directly affecting the roughness R_a and the surface topography.

Yi et al. [10] stated that they used SLM in the manufacture of Inconel 718 samples. The influence of the energy density of the laser was investigated

with values between 0.1 J/mm and 0.3 J/mm on the physical and mechanical properties of the samples. At the value of 0.2 J/mm there are few pores and good tensile strength: the fine striations are distributed on the laser-cut surface. The diffraction test revealed the presence of fine granules on the surfaces affected by the laser when the overlapping and stacking of the molten surfaces takes place. The results show that increasing the energy density results in distortions of the samples and the increase of the residual stresses.

Hatala et al. [11] have developed material laser cutting to improve manufacturing technology. This paper deals with the effect of the transverse cutting speed on the surface roughness when laser cutting of non-alloy structural steel. The experiment showed that the laser beam movement speed differs depending on the microgeometry of the cutting surface. Differences between the roughness of upper and lower surfaces were found. The difference in the quality of the lower- and upper-level separating areas is not noticeable and visible in the case of materials separated by a small thickness area. The cutting technology of non-structural steel is investigated by evaluating the effect of the crossing speed on the surface roughness.

Kim et al [12] show the influence of the assistant gas in the laser-cutting process on the quality of the cutting parts. The study is based on numerical analysis to predict and interpret the cutting tendency according to the nozzle design and the stand-off distance in order to improve the quality. In the cutting process, a conical nozzle and a supersonic nozzle were used with which numerical simulations were performed for a set of stand-off distances (nozzle-piece) using a Navier-Stokes model. Due to the similarity between flows, using the normal shock theory, the cutting tendency was analysed to predict the quality through a free-jet simulation.

Feng et al. [13] developed an analytical model that predicts the surface roughness of the Inconel 718 based on the kinematic description of the tool movements and the response of the machined part, elastically deformed due to milling forces. The milling experiments are performed by conventional laser-assisted milling with the cutting parameters run in seven different sets. It is found that the analytical model is a fast method to predict surface roughness in the milling process. The authors studied the Inconel 718 material, stating that it is a difficult material, and the products in this material require surface finishing. They compare analytical predictions with experimental results indicating high accuracy.

Masoudi et al. [14] show that in plasma cutting of 309 stainless steel, three output parameters, *Kerf*, R_a, *HAZ*, are critical factors affecting the efficiency and quality of the cutting. In their research, the effect of the input parameters, the current, the cutting speed and the gas pressure was tested to establish an understanding of the relationship between the input and output variables. The experimental data were used to develop three predictive models by intelligent systems based on the genetic algorithm (GA) and the artificial neural network (ANN). Finally, a hybrid technique of genetically optimized neural network (GONNs) systems was used to optimize process outputs. The experimental results showed that the current was the most sensitive variable among the investigated parameters.

1 METHODS AND EXPERIMENTAL

In this article, we proposed finding the mathematical formula of the roughness (R_a) increasingly used in research studies to increase the quality of the metal parts [15].

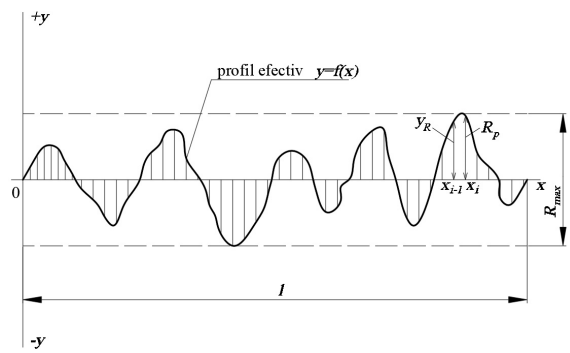

Fig. 1. *Graph of roughness (Ra) determination*

The roughness is defined as the arithmetic mean of the y_i values.

$$R_a = \frac{\sum_{i=1}^{k} |y_i|}{k}. \tag{1}$$

The curve of the graph surrounds an area equal to the sum of squares $y_1^2, y_2^2, \ldots, y_k^2$, over a reference length *l*. The area can be calculated:

$$y_1^2 + y_2^2 + \ldots + y_k^2 = \sum_{i=1}^{k} y_i^2 = \int_0^l y^2 dx. \tag{2}$$

The roughness R_a quantifies the set of irregularities that form the relief of the cut surface by using certain procedures.

A division of the interval $[0,l]$ is the point set $\{x_0, x_1, \ldots, x_n\} \subset [0,l]$ with the property:

$\Delta:(x_0<x_1<\ldots<x_i<\ldots<x_{n-1}<x_n)$, x_i divisions of $[0,l]$ interval,

$$x_i = i\frac{l}{n}, \tag{3}$$

and an arbitrary point: $\xi_i \in [x_{i-1}, x_i], 1=1,\ldots,n,$ where $f(\xi_i)=y_i$, and $\sum_{i=1}^{n} y_i^2 = \min$.

The Riemann sum on the interval $[0,l]$ is the area below the graph, that is:

$$\lim_{n\to\infty}\frac{l}{n}\sum_{i=1}^{n} y_i^2 = \lim_{n\to\infty}\frac{l}{n}\sum_{i=1}^{n} f^2(\xi_i) =$$
$$= \lim_{n\to\infty}\sum_{i=1}^{n} y_i^2(x_i - x_{i-1}) = \int_0^l f^2(x)dx = \int_0^l y^2 dx. \tag{4}$$

The area of the rectangle having the length $(x_i - x_{i-1})$ and the height $(y_R - R_P)$ is expressed by an integral.

Define:

$$R_a = \frac{\sum_{i=1}^{n}|y_i|}{n} = \frac{1}{n}\sum_{i=1}^{n}|y_i| = \frac{1}{l}\cdot\frac{l}{n}\sum_{i=1}^{n}|y_i| =$$
$$= \frac{1}{l}\cdot\sum_{i=1}^{n}|y_i|\cdot(x_i - x_{i-1})$$
$$= \frac{1}{l}\cdot\sum_{i=1}^{n}|y_R - R_p|\cdot(x_i - x_{i-1}) = \frac{1}{l}\cdot\int_0^l |y_R - R_p|dx. \tag{5}$$

According to fig.1, $f(x_{i-1}) = y_R$, $f(x_i) = R_P$.

R_i is the maximum height of the function f profile within a sample with length l in the direction of the axis Ox. The Riemann integral allows determining the roughness R_a starting from the Riemann sum. The roughness is calculated using the integrals using the property that the limit of the Riemann rows equals the integral from 0 to l. The roughness is finer as the area under the $|y_R - R_P|$ graph is smaller. The curve line describes the graph of the function f given by the equation:

$$R_a = \frac{1}{l}\int_0^l |y_R - R_p|\cdot dx. \tag{6}$$

The integral is approximated by the area of a rectangle with the base $x_i - x_{i-1}$ and the height $f(\xi)$ at the intermediate point $\xi \in x_i - x_{i-1}$, the function f being continuous.

The above-presented results from the theorem of the defined integral average:

$$\int_a^b f(x)dx = (b-a)f(\xi). \tag{7}$$

We have proposed a study of the roughness according to some input variables, the prediction and the correlation formula for R_a. As well, the hardness and the cutting width were studied when cutting with CO_2 laser parts of a steel material, less well-known in scientific articles, called HARDOX400 (H400).

Laser-cutting technology is used in industrial engineering to manufacture hard steel parts. It is a high productivity and profitability process.

The laser-cutting process, roughness optimization according to the laser input parameters and quality evaluation of the cut surfaces were studied in a number of papers. The influence of the laser-cutting parameters on R_a was studied by Mesko et al. **[16]** for S235JR steel, by Rao and Murthy **[17]** for stainless steel, by Adarsha Kumar **[18]** for AISI 4340 steel. Riveiro et al. **[19]** studied the interaction between the assistant gas and the part as well as the role of the nozzle on R_a for AISI 4340 steel. Spena **[20]** approached the influence of the cutting parameters on steel sheets used for car bodies. Hirano and Fabbro **[21]** studied the quality of thick steel sheets according to laser wavelength. Zlamal et al. **[22]** assessed the quality of S235JR steel, 10 and 15 mm thick, after the laser cutting. Lazov et al. **[23]** used the regression method to establish the cutting quality influenced by the cutting parameters. Wardhana et al. **[24]** observed that speed has the greatest influence on R_a for 316L stainless steel. Sharifi si Akbari **[25]** studied laser cutting for Al6061T6 alloy to determine the effects of the process parameters on the cutting zone temperature and cut edge quality.

We propose an analysis of the laser-cutting technology as follows: after irradiating steel material with light from a CO_2 laser, the incident photons collide with the valence electrons of the constituent atoms, they easily leave the electronic configuration, becoming free electrons, giving birth to the electronic cloud that moves through steel due to the conducting electrons that strike the metal network ions. At the place where the laser beam reaches the steel plate, the temperature is maximum in the centre, the order is 10^4 to 10^6 degrees Celsius, so that the ions of the network begin to vibrate very strongly due to the received heat, and the motion is transmitted to the neighbouring ions, which in turn start to vibrate giving rise to a damped oscillatory motion. In the steel sheet, the heat due to the vibration of the conducting ions and electrons having a wavy behaviour appears, the heat released by laser melting and the heat released by the burning reaction of Fe with O_2 is transmitted through the plate through the thermal conduction phenomenon. Of particular importance for laser-material interaction is the characteristics of the laser beam. For the CO_2 laser, the spot diameter used in the experiment is 0.2

mm. The spot has a spherical shape with the focal spot of microns placed in the centre. Laser cutting is the phenomenon of the thermal processing of metallic materials (HARDOX steel sheets) under the influence of a laser beam. The laser pulse lifetime is of seconds in continuous CW regime. Laser cutting is done by melting the material and removing it with O_2 jet. With the penetration of the laser in the H400 steel, the laser is pierced through a circular hole with a diameter of 0.3 mm to 1.25 mm and then cutting in a straight profile in the plate with the cutting width of 0.35 mm to 0.84 mm until it penetrates the contour of the part. In the stationary piercing regime, the material was pulled. The role of the assistant gas is to push the melt to the bottom of the sheet, to increase the volume of the piercing channel and to remove the melt on the upper and lower sides of the steel sheet. On the steel sheet surface, melt deposition surrounding the channel is noted. The assistant gas jet has kinetic energy that forces the melt and slag out of the cutting area. The incident intensity I_0 of the laser when cutting has a value in the range 10^5 to 10^6. By thermal heating, the material is brought to the melting temperature, forming due to the surface tension a melt in the form of an ellipsoid. The volume of the portion heated to the melting temperature T_m forms the liquid melt. The melt in the liquid state is heated until it reaches the laminar flow state at the melting temperature of Fe due to the laser source and the oxygen assistant gas. Removal of the cut material is done in a liquid (molten) state, in addition to the laser radiation, the oxidation reaction: $Fe + O \rightarrow FeO + Q$ takes place, which is an exo-energetic reaction with the release of Fe oxides.

The evaporation energy of the melt is equal to the energy of the melt minus the binding energy of the metal electrons. The cutting process is characterized by the penetration of the material and the occurrence of the oxidation reaction. The mechanism of liquid melt removal by CO_2 laser consists of the absorption of photons by the metal surface, transforming the light energy into caloric energy, local melting of the surface with melt formation, removing the melt when the temperature in the centre reaches the melting and vaporization temperature, with the help of compressed oxygen gas, which eliminates particles from the cutting area through an incandescent flow. The cutting has the following constituent subprocesses: sublimation of a small amount of material that is heated to the vaporization temperature T_v, the vapours being evacuated by the compressed gas, elimination of a quantity of the molten material in the channel by a stream of incandescent drops at the melting temperature T_m by the cutting gas, oxidation of Fe in the presence of oxygen giving rise to fine solidified droplets on the lower edge of the cut along the contour of the part separated by the plate, the reaction being more intense towards the lower edge, thus resulting in a higher cutting speed. The role of oxygen is to remove the molten material, trigger and maintain the Fe oxidation reaction, but also to protect the focusing lens L. Purity of O_2 is 99.97 %. It directly influences combustion and cutting speed. The cutting surface of the material is formed by a melted and resolidified layer due to the cooling of the piece. In laser cutting, the distance between the nozzle and the part is important because the laser beam and CO_2 gas are co-axially transmitted to the workpiece. The parameters used in the cutting are: the distance between the nozzle and the cutting area: 0.8 mm, the focal position: –0.5 mm inside the piece, the radius of the correction instrument: 0.3 mm. The reflection degree of the H400 steel is low, which makes it easier to cut. The low thermal conductivity delays the diffusion of heat through the material, which helps the local melting made by the laser.

Using the laser installation, the accuracy is better than in any plasma and oxygen cutting, the laser cutting time is lower, and the quality of the cut surface is significantly higher, the roughness close to the roughness obtained by chip removing process, the profitability is higher than in the case of cutting with plasma or oxygen. An analysis of the surfaces reveals uniform oscillations of level, not detectable by the human eye appear, following the evacuation of the melt from the slit. Incandescent liquid drops can give rise to striations and pores on the surfaces affected by the laser. After laser cutting, the material decomposes into a liquid phase and a vapour phase. All these compete for a much shorter processing time compared to plasma or oxygen cutting, small melting mass, reduced amount of lost material.

In this way, technological additions for the part design and manufacturing can be substantially reduced, the use of the semifinished part is more profitable, and the loss of material being incomparably smaller.

The pollution of the environment is reduced due to the small slot, short cutting time, material saving, reduced maintenance factors, and a much longer service life of the machine compared to the other two processes. One of the benefits of this operation is that the laser cutting does not change the chemical composition. HAZ is much diminished in comparison to the other two procedures. This cutting process does not influence the flatness, rectilinearity, or shape of

the semi-finished product. The number of products obtained per hour with laser technology is much higher than in other processes.

The laser beam has a circular section; depending on the diameter D before focusing, it can be defocused with $\pm\Delta f$. Defocusing has effects on the material melting and, for steel, it is recommended that this one be inside the material. With the focus inside the material, a decrease of the intensity at the surface of the piece results, the size of the focal spot will increase resulting in the increase of the interaction time between the laser and the material, and thus also the R_a value. In the case of thick steel cutting, for a good cutting, it is necessary that the area of parallelism of the beam z be small, that is, the maximum intensity I_0 being kept constant, the melting depth z_m being correlated with the diameter of the spot d. The laser spot plays an important role in laser cutting, because beneath it a heated portion of a convex plane shape is produced at the beginning, then, by heating, the plane-convex or biconvex melt and the heated convex meniscus shaped surface under it are formed, and finally the melt and heated area are elongated by heating, resulting in vaporization. The increase of the laser power has the effect of increasing the laser intensity, thus the melting occurs, and if the intensity increases further, the vaporization of the material results. The intensity of the laser beam depends on the radiation energy, and for linear contour cutting a linear energy E_l and a melting energy E_v are necessary. If the cutting speed of the laser increases, the time of interaction between the laser and the material decreases, which implies smaller dimensions of the molten and heated area, less material melted, reduced time of melt elimination with the help of cutting gas, thus leading to better cutting and melting efficiency. The melt is ejected partially on the sidewalls of the cut surfaces. By eliminating the melt its mass decreases and the roughness is better at the bottom than at the upper area, because by the movement of the melt and of the hot drops of liquid, a series of formations are resulting on the cut surface: striations, irregular or inhomogeneous surface, and the oxide film will cover all this. The number, size, and density of the striations increase with the thickness of the steel.

A variable describing the interaction of laser radiation with the processed steel part is the focused radiation energy, defined by the mathematical relation:

$$E = \frac{4P}{\pi \cdot t_i \cdot f^2 \cdot \theta^2}, \tag{8}$$

where P is a laser power, t_i interaction time, f convergence distance of the lens, and θ beam divergence.

The cutting efficiency is defined as the ratio between the surface cut in a second and the energy developed by the laser in 1 second (the surface cut with the power of 1 J):

$$\sigma_{CUT} = \frac{v \cdot g}{P}, \tag{9}$$

where v is laser speed, g material thickness, and P laser power.

The cost parameter defines the cutting speed obtained with a certain laser power:

$$C_{CUT} = \frac{v}{P}, \tag{10}$$

Laser-cutting efficiency is defined as the ratio between cutting efficiency and cost parameter:

$$T_m = \frac{P}{k_t \cdot d}, \tag{11}$$

The efficiency is good if the cutting speed / laser power ratio is lower, i.e., low speed cutting and high laser power.

The temperature at the surface of the material can be calculated by the expression:

$$T_m = \frac{P}{k_t \cdot d}, \tag{12}$$

where k_t is a thermal conductivity of the material, and d diameter of the focused beam or the laser spot.

The vaporized mass can be easily deduced as the mass of the molten material from the slot minus the molten mass of oxides found as slag in the waste tray below the grill of the installation:

$$m_v = \rho \cdot V_{topit} - M_{oxizi} = \rho \cdot \overline{K_{kerf}} \cdot g \cdot l - M_{oxizi}, \tag{13}$$

where V_{topit} is a volume of the melt, l length of the contour of the cut piece, g material thickness, $\overline{K_{kerf}}$ average width of the cut, and ρ density of the melt.

For laser thermal cutting, we used a steel plate made of H400, 10 mm thick, with a length of 475 mm and a width of 265 mm, which has a content of: 0.19 % carbon, 1.25 % manganese, 0.70 % chromium, 0.38 % molybdenum, 0.50 % silicon.

Initially, we prepared a reduced factorial experiment, involving Taguchi's method for the H400 steel plate. Thus, we made the plan of cutting 45 pieces (Fig. 2). A piece was built with three linear sides and a circular one for CO_2 laser cutting. Geometrically, a piece is inscribed in a 40 mm side square.

Currently, no research available in the literature has been found that describes the dependence of the roughness on the influence parameters of the process

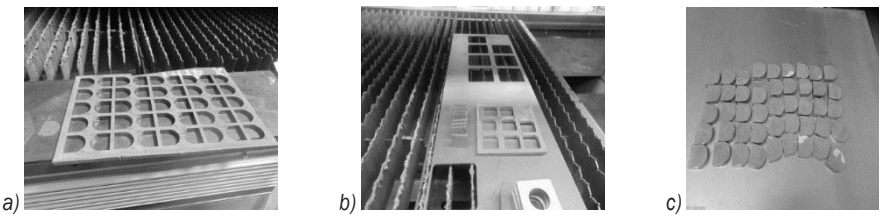

Fig. 2. *a) Sample plate, b) H400 plate, and c) cut parts*

when cutting Hardox laser plates. In this context, the objective of the research is to determine in what way the roughness of the surface processed by laser cutting is influenced by the input parameters of the process and what the correlation formula between them is. Thus, we aim to obtain a mathematical formula, the dependence of the roughness on the influencing parameters when at least two parameters act simultaneously, and one is kept constant, using the ANOVA regression model.

In a preliminary research, we identified the limit values of the selected parameters for which cutting can exist (at too low laser power, the beam does not pierce the 10 mm thickness H400 plate).

The optimum cutting speeds, the assistant gas pressure, and other cutting parameters are specified in Table 1.

Table 1. *Description of the cutting parameters*

General parameters	Value	Unit of measure
Group	STAHL	
Material	STW22	-
Plate thickness	10	mm
Cutting mode	Contin. regime	CW
Max. laser power	4.400	W
Lens with focal length	190.5	mm
Nozzle type	NK1515	
Focal position	-0.5	mm
Nozzle diameter	1.5	mm
The nozzle-piece distance	0.8	mm
Assistant gas	O2	-
Cutting speed I	1.200	mm/min
Cutting speed II	1.400	mm/min
Cutting speed III	1.600	mm/min

In the experiment we have as varied parameters: laser power (P), pressure of the assistant gas (p), laser cutting speed (v) with the values as it follows: power, P_1 = 4100 W, P_2 = 4200 W, P_3 = 4300 W; pressure of the assistant gas, p_1 = 0.35 bar, p_2 = 0.45 bar, p_3 = 0.55 bar, and cutting speed, v_1 = 1200 mm/s, v_2 = 1400 mm/s, v_3 = 1600 mm/s (Table 2).

The references from the reduced factorial plan were replicated four times in order to carry out the statistical research observations regarding the study of R_a roughness.

Table 2. *Reduced factorial experimental plan*

No. Part	Power [W]	Pressure [bar]	Speed [mm/min]
1	4100	0.35	1200
2	4100	0.45	1400
3	4100	0.55	1600
4	4200	0.35	1400
5	4200	0.45	1600
6	4200	0.55	1200
7	4300	0.35	1600
8	4300	0.45	1200
9	4300	0.55	1400

The investigation of the technological cutting process is focused on modelling to investigate the process accurately. Experimental modelling establishes the correlation between the input parameters, called the influence factors, and the values measured by different procedures using the measuring instruments. The experiment used a factorial array/matrix that uses the combination of variable levels, i.e., 3^3. The minimum level has the logical value –1, the average value 0, and the maximum level has the logical value +1. In order to find the coefficients of a polynomial that contains the influencing factors and the products between them, which signify the interactions between these factors, a number of 3^2 = 9 tests were performed. The optimization algorithm starts running after establishing the extreme values of the parameters presented in Table 3.

Table 3. *Input parameters and their extreme values*

Parameters	Minimum	Maximum
Laser power [W]	4100	4300
Speed [mm/min]	1200	1600
Gas pressure [bar]	0.35	0.55
Focal position [mm]	–0.5	–0.5

A series consists of three references: S1: 1, 2, 3; S2: 4, 5, 6; S3: 7, 8, 9.

In the case of the first factorial series, the power is kept constant at the value of 4100 W and the pressure changed by +0.10 bar from the value of 0.35 bar, and the speed increased by 200 mm/min starting with the value of 1200 mm/min. The second series is obtained according to a certain rule by modifying and increasing the power by 100 W to the value of 4200 W, the pressure changed by +0.10 bar, from the value 0.35 bar to 0.45 bar and 0.55 bar, and the speed modified with 200 mm/min starting with the value of 1400 mm/min. The third series is obtained according to a certain rule by modifying and increasing the power by 100 W to the value of 4300 W, the pressure changed by +0.10 bar from the value 0.35 bar to 0.45 bar and 0.55 bar, and the speed changed by 200 mm/min, starting with the value of 1600 mm/min. The three factorial series are replicated four times to the same values according to the above-described model.

Previously, the authors studied the laser-steel material interaction, considering that when the laser beam enters the material, it enters a diameter of d = 0.2 mm. The wavelength of CO_2 laser radiation is λ = 10.6 μm. The beam diameter before focusing is D = 20 mm. The beam divergence angle is calculated by the Rayleigh formula:

$$\theta = 1.22\frac{\lambda}{D}. \tag{14}$$

Calculating with the above values, we obtain θ = 0.64 mrad.

Radiation power equals the ratio of radiation energy E to laser duration τ:

$$P = \frac{\mathrm{E}}{\tau}. \tag{15}$$

Radiation intensity in focal spot:

$$I_0 = \frac{P}{S} = \frac{\mathrm{E}}{S\cdot\tau} = \frac{E}{\frac{\pi d^2}{4}\cdot\tau} = \frac{4\mathrm{E}}{\pi\tau d^2}. \tag{16}$$

We can describe the interaction between radiation and material as follows, in Fig. 3.

The reflected beam is RI_0 and depends on the reflection coefficient of the material. The beam that penetrates the material has an intensity dependent on the penetration depth and decreases after the gradient $\partial I / \partial z$ as z increases:

$$I = (1-R)I_0 e^{-\mathrm{A}\cdot z}. \tag{17}$$

The intensity of the radiation that has entered the material decreases according to an exponential law, where R is the reflection coefficient and A is the absorption coefficient.

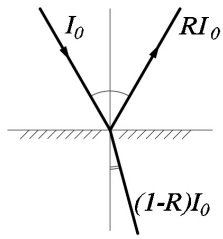

Fig. 3. *Interaction between laser radiation and substance*

It must be known that surface roughness influences the absorption of laser radiation.

2 RESULTS

The surfaces of the laser-cut H400 steel parts are subjected to a heat treatment. In the place where the laser radiation meets the surface of the material, the temperature is maximum. Iron is heated to the result of the Feα-magnetic 20 °C to 750 °C, Feα-non-magnetic 750 °C to 913°C, Fe ϒ 913 °C to 1390 °C, at 1200 °C iron ignites in the presence of O_2 in an oxidation reaction, Fe δ 1390 °C to 1537°C, liquid iron 1537 °C to 3000 °C, vaporized iron >3000 °C. After the laser action stops, iron is suddenly cooled. The heating temperatures do not coincide with the cooling temperatures; the difference between them gives us the thermal hysteresis. By fast cooling, the steel surface is hardened. It can be improved by metal alloying.

In the experiment, we initially located on the test plate the point where the cut piece has the best quality given by the combination of parameters: laser power, cutting speed and gas pressure. Based on this determination, the experiment was subsequently designed.Of course, the piece interacts with the geometry of the conical beam which determines the geometry of the cutting slot.

One aspect to note for the beam is that it does not have the same intensity at all points, the distribution being given by the Gaussian curve. The incident intensity I_0 is calculated in Table 4. The quality of the material is also given by the chemical composition, a higher concentration of carbon and manganese ensures a surface with low roughness, because carbon and manganese burn well in the presence of oxygen. In contrast, we cannot say the same thing about silicon, it melts harder and produces irregular surfaces (craters, pores. etc.). In order to obtain the roughness of the surface, the liquid melt plays a decisive role. Its

shape is given by the surface tension. In the centre of the melt, the temperature is maximum, and it drops to the edges due to the temperature gradient.

Table 4. *Radiation intensity I_0 for H400 parts*

Parameter	Exp. 1	Exp. 2	Exp. 3
Laser durat. CW (τ), [s]	$\tau_1 = 14$ s	$\tau_2 = 13$ s	$\tau_3 = 12$ s
Power, [W]	4100	4200	4300
Radiat. ener. (E), [J]	57.400	54.600	51.600
Radiat. intensity I_0, [W/cm^2]	9.76×10^5	10.76×10^5	14.33×10^5

It follows that in the droplet, a displacement of liquid metal occurs from the focal point towards the edge, which gives us the concave shape of the droplet. This is removed from the channel with the assistant gas jet blowing and breaking the drop into two fronts containing liquid metal droplets that are ejected through the bottom edge of the plate. The molten droplets give rise to striations, and the craters are formed due to the oxidation reaction and appear on the oxidized surface. By cooling, the solidification of the slit surfaces takes place, resulting in a relief with irregularities. giving rise to the appearance of roughness.

From the results of the cutting experiment (Table 5), it is found that the cutting width increases at the bottom, this shows the conicity of the piece at each reference $W_i > W_s$. This result is important because the molten mass increases at the bottom, so the number of molten drops also increases due to the oxidation chemical reaction. The best cutting values in the initial experiment are at a minimum power of 4100 W and maximum values of pressure and speed, $Ws = 0.6220$ mm. The same result is obtained at part no. 39. For the measurement of the parts, an electronic micrometer was used.

Hardness was measured with a Krautkramer MIC 2V durometer. The part hardness is given by the high concentration of carbon, which are higher concentration results in higher hardness. For the HARDOX material, hardness varies from the initial value of 29 HRC. The hardness of the piece in the initial experiment is maximum for piece 1, which is 30.80 HRC, so at the minimum values of the power which is 4100 W, the pressure of 0.35 bar and the speed of 1200 mm/s. Subsequently, after heating the material and transmitting heat to the plate, the hardness randomly varies with smaller values obtained compared to part 1, which does not comply with a calculation formula.

The lowest hardness value is 23.90 HRC and occurs at maximum power, maximum speed and minimum pressure. The best hardness is obtained for parts 11 and 27 of 31.60 HRC made at low power, medium pressure and speed, respectively at maximum power and pressure and average speed.

The roughness was measured in the laboratory of Constantin Brancusi University with a Mytutoyo rugosimeter. The minimum value of R_a 1.7 μm, is obtained for the 45 pieces at the average value of pressure and maximum cutting speed when the power is kept constant at the value of 4200 W.

The graph in Fig. 4 shows a variation of the hardness according to R_a for the proposed experiment. The maximum hardness values are obtained for R_a in the range of 2 μm to 3 μm.

From Fig. 5 it follows that at higher values of R_a we obtain lower values of density. The measured HRC points can be approximated by a sine function.

Table 6 presents the statistical data obtained by running the program referring at the average roughness and the standard deviation of the roughness as well as the value of the limit coefficients (upper and lower).

Table 6 shows Design 3^3 with 3 levels of laser power variations, assistant gas pressure, cutting speed,

Table 5. *Values of the measured parameters; the width of the cut up-down, hardness, roughness (replica no. 4)*

Experiment No.	No. crt Ref.	Laser power [W]	Gas press. O_2 [bar]	Cutting speed [mm/min]	Kerf-W_s [mm]	Kerf-W_i [mm]	Hardness down part [HRC]	R_a [μm]
Replica 4	37	4100	0.35	1200	0.5755	0.6880	28.00	3.26
	38	4100	0.45	1400	0.6575	0.6750	30.10	2.87
	39	4100	0.55	1600	0.6720	0.6765	27.60	2.56
	40	4200	0.35	1400	0.5595	0.6870	28.10	2.09
	41	4200	0.45	1600	0.6495	0.6500	28.20	3.46
	42	4200	0.55	1200	0.6430	0.7615	28.10	4.05
	43	4300	0.35	1600	0.5755	0.6865	28.30	3.75
	44	4300	0.45	1200	0.7015	0.7295	29.90	2.56
	45	4300	0.55	1400	0.6895	0.6980	27.30	3.63

1 block with 45 operated parts where the roughness R_a was measured. The DOE took into account an experiment reduced to 9 observations, replicated at the same points four times. The central point of the experiment was chosen after testing on the H400 test plate at P = 4200 W, p = 0.65 bar, v = 1400 mm/min.

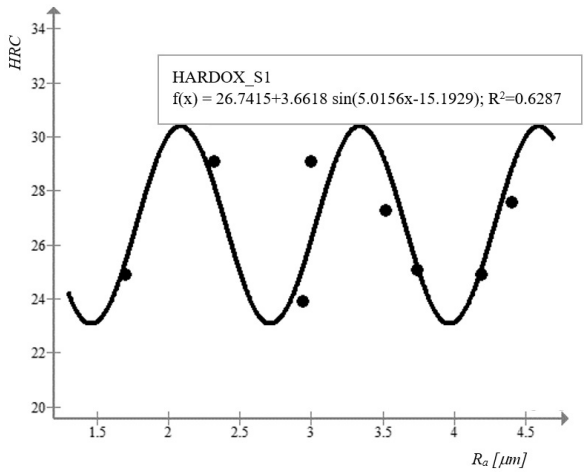

Fig. 4. *Variation of hardness depending of the roughness R_a for the initial experiment*

The minimum and maximum levels were chosen for the input parameters with ±100 W for laser power P_M = 4300 W, P_m = 4100 W, ±0.10 bar for the cutting gas pressure p_M = 0.55 bar, p_m = 0.35 bar, the speed of laser cutting ±200 mm/min, v_M = 600 mm/min, v_m = 1200 mm/min. These values varied according to the following rule: The power was maintained constant at 4100 W and the pressure was run at the minimum, average, maximum value (0.35 bar, 0.45 bar, 0.55 bar) and laser-cutting speed at the value minimum, average, maximum (1200 mm/min, 1400 mm/min, 1600 mm/min). The power was increased to the constant value of 4200 W and the pressure was run to the minimum, average, maximum value (0.35 bar, 0.45 bar, 0.55 bar), respectively: the speed was increased by 200 mm/min from the value 1400 mm/min, 1600 mm/min, 1200 mm/min. The power was increased to the constant value of 4300 W and the pressure was run to the minimum, average, maximum value (0.35 bar, 0.45 bar, 0.55 bar), respectively the speed started from 1600 mm/min, after which it ran at 1200 mm/min and at 1400 mm/min. The average roughness was calculated for 5 parts run under observation conditions 1, technologically obtained under the same conditions, and was found:

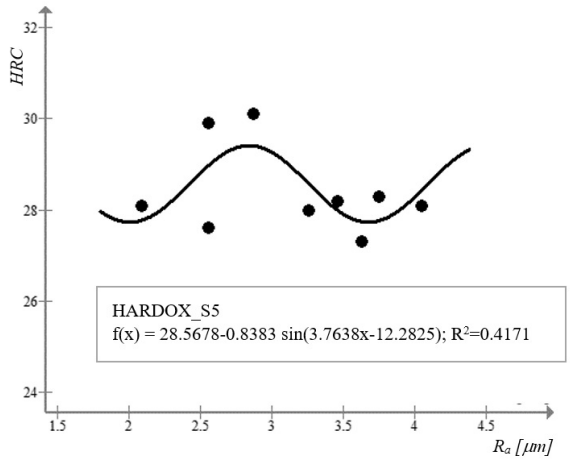

Fig. 5. *Variation of hardness depending of the roughness R_a for Replica 4*

Similarly, it is calculated for the other series resulting in a column the average of 3.4142 for the roughness of the 45 pieces. For the standard deviation, the classical formula for n = 5 is applied, and carrying out the square sum SS, a standard error of 0.3812 results for series 1. Calculating the roughness average in the column, summing all the values and averaging

Table 6. *Statistical data referring to the independent variables and dependant variable: mean and standard deviation (mean square deviation)*

Design: 3 3-level factors, 1 Blocks, 45 Runs (Rugosity)								
	Power [W]	Pressure [bar]	Speed [mm/min]	Rugosity – Means [μm]	Rugosity - Std. Dev.	Rugosity – N	-95,% - Cnf.Limt	+95,% - Cnf.Limt
1	4100	0.35	1200	3.2780	0.3812	5	2.8046	3.7513
2	4100	0.45	1400	2.9920	0.5495	5	2.3096	3.6743
3	4100	0.55	1600	3.4580	0.7853	5	2.4828	4.4331
4	4200	0.35	1400	3.1180	0.8537	5	2.0579	4.1780
5	4200	0.45	1600	2.8520	0.8366	5	1.8131	3.8908
6	4200	0.55	1200	4.3360	0.8347	5	3.2994	5.3725
7	4300	0.35	1600	3.5120	0.5962	5	2.7717	4.2522
8	4300	0.45	1200	3.8420	0.8521	5	2.7838	4.9001
9	4300	0.55	1400	3.3400	0.2440	5	3.0369	3.6430
All Runs				3.4142	0.7624	45	3.1851	3.6432

the roughness values for all the parts. we find the value 3.4142 micrometres for the whole block. In the column of standard deviation for roughness, we have the standard error values for each series 1 to 9 resulting in an average square error of 0.7624. $N = 45$ represents the rank of the block.

$$\bar{R}_a = \frac{3.48 + 3.81 + 2.94 + 2.90 + 3.26}{5} = 3.2780. \quad (18)$$

We can calculate the confidence limit, taking into account the confidence interval $Z = 1.96$

The calculated in the table data, respectively the average roughness, Z, standard deviation, the mean of the standard deviation with $n = 5$, will be taken into account. With these values, we can easily calculate the t-student distribution for eliminating aberrant values. The R_a values distributed as a Gauss bell are found in the interval t and $-t$. Error distribution, probability p is made in the range –95 % and $-t$, respectively t and +95 %.

3 DISCUSSION

Response surfaces (RSM) are study methods that indicate results in an accessible form. RSM presents a 3D graph of the measured value R_a based on two influence factors. With the help of the Statistica.7 software, the correlation formula between the influencing factors was established. The interaction between the influencing factors describes the hierarchy of the interactions between them. There is statistical software in which the influence factors in real values are used in the approximation of the correlation formula (SI), resulting in the comparison. The magnitude of the effect of a parameter is given by the polynomial coefficient module.

1. Prediction: Vary power and speed, pressure remains constant,

a. For surface plot (fitted response):

The graph shows that at high cutting speeds 1550 mm/s to 1600 mm/s low values of roughness $R_a < 3$ µm are obtained when the laser power is 4080 W to 4120 W. and its high values are obtained when the speeds are low, so when the laser stays longer in the material by strongly heating the plate and the cut pieces. In this case, it can be observed that the lowest values of the roughness are obtained at low powers.

At low speeds and laser power near maximum, the roughness R_a increases over 4 µm. The prediction indicates the colour distribution according to the roughness values for the contour plot and shows that the variation of the laser speed and power is inversely proportional. R_a increases linearly with the decreasing of cutting speed and the increasing of laser power. The graph shows the measured values of R_a using the

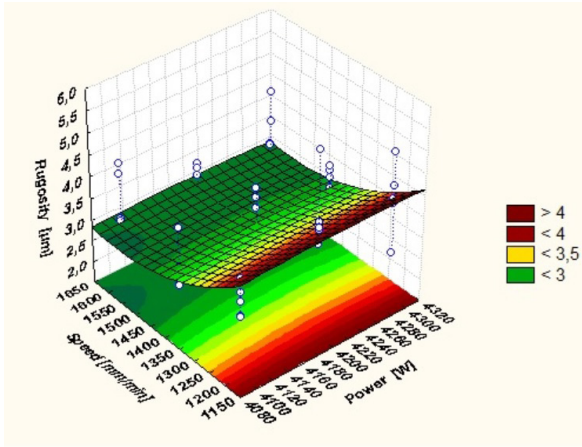

Fig. 6. *The influence of laser power and pressure on the roughness of the piece when the pressure is constant for surface plot (fitted response)*

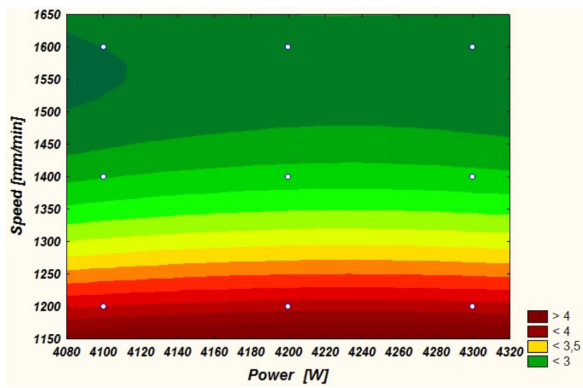

Fig. 7. *The influence of laser power and pressure on the roughness of the piece when the pressure is constant for contour plot (fitted response)*

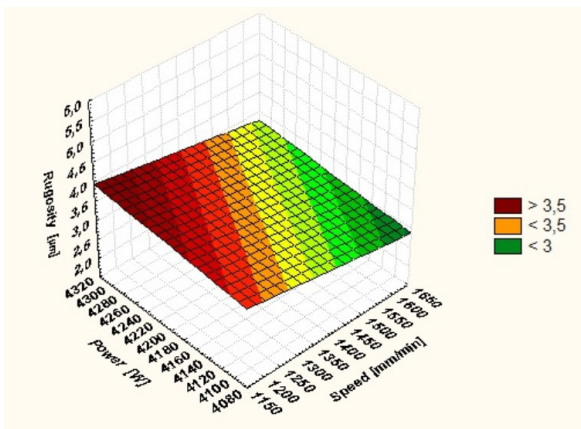

Fig. 8. *Machining the surface roughness against power and speed with the linear model*

SSM method through a fixed response. Using quadric SSM, we indicate R_a which is simultaneously under the influence factors speed and laser power.

b. For contour plot (fitted response).

2. The correlation formula of R_a when the factors of influence power and speed vary, and the pressure remains constant.

Correlation formula for the linear model (where X is speed, and Y power):

$$R_a = -1.4414 - 0.0014X + 0.0016Y. \quad (19)$$

R_a is small at high cutting speed and low power value, $R_a < 3$ μm. R_a is maximum for low speed and high laser power. The formula shows the increase of R_a under the more pronounced influence of the laser power. which has the coefficient of the higher influence factor. The result given by linear model is in accordance with the prediction. The result indicates that the predominant factor is power.

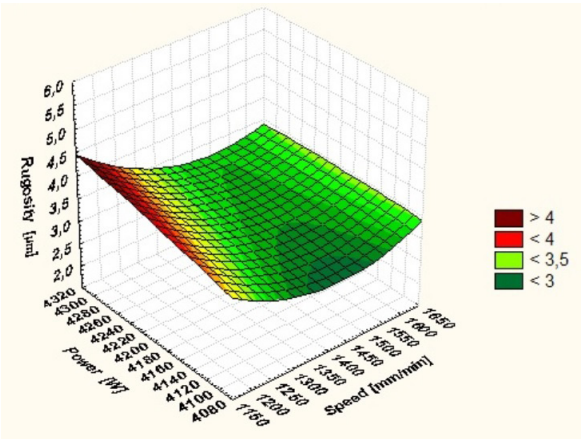

Fig. 9. *Machining the surface roughness against power and speed using the quadric model*

$$R_a = -75.0092 - 0.0023X + 0.0371Y + 9.9083E - \\ -6{\cdot}X{\cdot}X - 6.375E - 6{\cdot}X{\cdot}Y - 3.1667E - 6{\cdot}Y{\cdot}Y. \quad (20)$$

For expressing R_a as a function of two variables X, Y (laser power and speed), we used the quadratic polynomial model containing all the lower-order hierarchical terms, terms to be added to the model involving interactions, quadratic terms with regression coefficients. The equation defines the response surface, which is how R_a depends on X and Y, which is a surface in a multidimensional graph. In the equation above, E is a mathematical constant.

DOE avoids problems caused by correlated predictors. The coefficients can be obtained for calculating effects and interactions. The graph shows the curvature due to each variable X and Y for the designed experiment. The quadric model is a complete model completing the linear model that does not fit the data. Both models are mounted and analysed in the same way. The modulus of the correlation coefficient means that the order of influence is: 1. laser power, and 2. speed.

Eq. (20) indicates a pronounced dependence when the factors of influence speed and pressure interact with each other, but also of the dependence given by the quadratic coefficients for speed and power respectively. The graph shown by the correlation formula indicates that the best roughness R_a is obtained at average speed values, when the speed decreases between 1500 mm/min to 1400 mm/min and the laser power increases from 4100 W to 4140 W. R_a changes increases according to Gauss bell maintaining the speed between 1400 mm/min and 1500 mm/min but increasing the laser power from 4200 W to 4300 W using the quadric model. The influence due to the linear coefficients in the quadratic polynomial formula of R_a is very small in comparison to the quadratic coefficients due to the interaction with each one, respectively with the coefficient due to the interaction between the influence factors (speed and power). The coefficient of the linear power term is greater than the speed. The coefficient of the model indicates a decrease of the roughness R_a with a value of 75.0092. The result consists of identifying correlations that include the variations of the influencing factors that approximate the values of the measured parameters obtained from the experiment and which contain factorial series, giving rise to a mathematical model of prediction and establishing the correlation function. It is found that the prediction is in accordance with the correlation formulas of R_a.

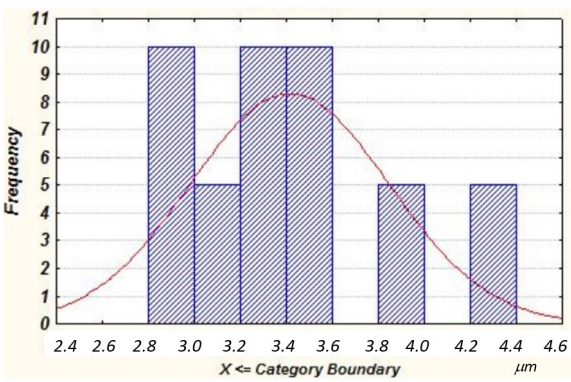

Fig. 10. *Histogram of predicted values. 3 3 level factors, 1 Blocks, 45 Runs; MS Residual =0.48123*

Analysing the histogram, the prediction of the roughness values R_a is shown in Fig. 10 with the arithmetic mean of 3.4 and a standard deviation of 0.7624. *X* category represents the measured value of R_a.

The histogram of the frequencies derives from the values of the pieces $n = 45$, determinations with a R_a of minimum 2.8 and maximum 4.4, the distribution of these values being slightly asymmetrical, this being due to the cutting defects (striations, pores etc.).

There are six intervals, with the following frequencies of appearance of the predicted R_a values: in the range (2.8 μm to 3.0 μm) there are $n_1 = 5$ values; in the range (3.0 μm to 3.2 μm) there are $n_2 = 5$ values; in the range (3.2 μm to 3.4 μm) there are $n_3 = 8$ values, in the range (3.4 μm to 3.6 μm) there are $n_4 = 8$ values, in the range (3.8 μm to 4.0 μm) there are $n_5 = 5$ values and in the range (4.2 μm to 4.4 μm) there are $n_6 = 2$ values. Most R_a values are grouped in the interval (2.8 to 3.6), close to the average.

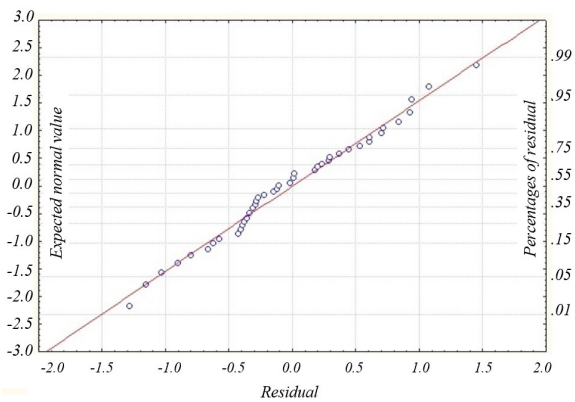

Fig. 11. *The graph of the linear regression of the normal values expectations as function of errors*

From the graph, one can observe that not all error data points are on the line, most error points are. The total sum of squares that are not on the line, explained by the linear regression model, is the residual sum of squares. In the case of the experiment, the average of the sum of residual squares is $MS_R = 0.48123$.

Table 7. *Final statistics*

λ	SSEI	χ^2	p
0.719563	17.19110	0.347263	0.555671

Table 7 shows the statistical coefficients of the errors for the measurement of the dependent variable, R_a. From Table 7, it follows that the standard error mean is 0.48123.

Significance test χ^2 Pearson indicates the association of columns and lines of a table with two entries: cutting speed and laser power. For our case, the significance of the association is 0.347263. Test χ^2 shows whether or not the two variables are independent. Finally, a comparison can be made between the significance test χ^2 (calculated) and the critical test χ^2, if there is a connection between speed and laser power. So, we can see that $0.347263 < 0.48123$, H0 (the null hypothesis) results, i.e. there is no significant link between the speed and the laser power, independent variables *B* and *C*.

λ coefficient is a measure of prediction error decreasing when the independent variables are known, power and speed.

$\lambda = 0.719563$, a value between 0 and 1, so the standard error can be estimated depending on the standard deviation and the root of the block rank *n*, where the coefficient λ is better the higher its value. The statistics are asymmetric, where the dependence variable is R_a. The coefficient λ called Goodman and Krushkal measures the reduction of the R_a error in the analysis of crossings for the laser power and cutting speed factors.

SSEI = 17.19110 indicates the sum of the squares of errors.

Test *p* indicates that the probability of errors is 0.555671, which is the probability of making an error. As $p > 0.05$ shows that the statistical connection is insignificant, the power and the speed do not have links between them, i.e., they are independent, so the probability of making an error is quite high.

4 CONCLUSIONS

In this article the roughness R_a of the part surface was studied, in the case of laser cutting of an H400 steel sheet. CO_2 laser-cutting experiments were performed with the following input cutting parameters: laser power 4100 W to 4300 W, oxygen pressure of 0.35 bar to 0.55 bar and cutting speed of 1200 mm/min to 1600 mm/min. The output parameter was the roughness of the surfaces resulted in the cutting process.

Experimental data were statistically analysed by using Anova from Statistics 7.0, in order to establish the linear and quadratic correlation formulas between the influence factors: power, speed, and constant pressure on the one hand and roughness on the other and to determine the predictive model, as well.

The main conclusions of the research are:

- Following the data processing, the quadratic predictive model shows that at high speed and at low laser power values, low values of roughness,

below 3.0 μm, are obtained, while in the linear predictive model, even if the power increases, the roughness is maintained at same value if speed does not vary.

- Using the quadric SSM model, the correlation between R_a and the two factors of influence (speed and laser power) is obtained. Thus, it can be concluded that at medium speed and low power, the roughness is improved (low values), and at low speeds and high laser power results high values for R_a.
- Using the linear SSM model, we obtain the correlation between R_a and the two factors, speed and laser power, proving that the roughness R_a has low values at high speeds and low power, and high values at low speed and high power.
- It is also deduced from the cutting experiments of the H400 material as well as from the formulas for determining the roughness R_a, that laser power is the most sensitive input parameter.
- Increasing laser power results in an increase of the laser focusing energy; therefore, the heat received by the material has the effect of increasing R_a and, for this reason, the minimum value of the laser power is recommended in order to obtain a low roughness value.
- R_a presents a relatively good agreement between the regression model and the predictive model.
- The representation of the quadric model indicates the variation of the investigated factors of influence, speed and power according to Gauss's function. R_a is minimum at average values of speed and at the lowest power. One explanation would be that the number of drops increases towards the lower part of the H400 steel plate, due to the oxidation reaction, resulting from the increase of the molten mass. R_a increases with the elimination of hot drops that give rise to an irregular surface. As the power increases, R_a increases, which is a coefficient of influence that establishes the hierarchy in the correlation formulas.
- The result of the interaction between the influence factors delimits the degree of roughness of the surface indicated by the intensity of the colour green. From the separate graphical analysis of the quadric model, we can see that R_a varies directly proportional to the laser power and exponentially with the speed. Outside the bell, the roughness increases exponentially with speed for parts that do not require further processing.
- By elongating the dependence curve between power and speed, the peak of the Gauss bell moves to higher values of roughness. This means that the temperature inside the slot has increased. Therefore, it is recommended to use minimum power and medium speed for the critical parts of the piece with the potential to be damaged.
- For a better understanding of the relation between power and speed, we propose equating the linear relationship with the quadratic one in order to observe this dependence, which must be an exponential function. If the exponent of the relation grows, the peak of the bell moves towards a larger R_a. The area of the figure below the graph shows the level of roughness of the surface.

The values used in the experiment can be considered optimal for the cutting machine operator and the process engineer when they target the roughness of the cut part surfaces. For example, to achieve a cutting roughness under 3 μm and for 10 mm thickness of material, the laser power value should be 4100 W while the cutting speed should be 1400 mm/min, at a low, constant, gas pressure.

5 ACKNOWLEDGEMENTS

Thank you to the manager Radu NUȚU and the laser machine operator Liviu from Brașov for their technical support in conducting this CO_2 laser experiment.

6 REFERENCES

[1] Adelmann, B., Hellmann, R. (2011). Fast laser cutting optimization algorithm. *Physics Procedia*, vol. 12 p. 591-598, **DOI:10.1016/j.phpro.2011.03.075**.

[2] Lutey, A.H.A., Ascari, A., Fortunato, A., Romoli, L. (2018). Long-pulse quasi-CW laser cutting of metals. *International Journal of Advanced Manufacturing Technology*, vol.94, p 155-162, **DOI:10.1007/s00170-017-0913-x**.

[3] Ivarson, A., Powell, J., Siltanen, J. (2015). Influence of alloying elements on the laser cutting process. *Physics Procedia*, vol. 78, p. 84-88, **DOI:10.1016/j.phpro.2015.11.020**.

[4] Pocorni, J., Powell, J., Frostevarg, J., Kaplan, A.F.H. (2018). Dynamic laser piercing of thick section metals. *Optics and Lasers in Engineering*, vol. 100, p. 82-89, **DOI:10.1016/j.optlaseng.2017.07.012**.

[5] Shulyatyev, Victor B.; Orishich, Anatoly M., (2018), Microcraters and surface quality in laser oxygen cutting of thick steel sheets. *Journal of Laser Applications*, vol. 30, no. 2, art ID 022003, **DOI:10.2351/1.5008798**.

[6] Thombansen, U., Hermanns, T., Stoyanov, S. (2014). Setup and maintenance of manufacturing quality in CO_2 laser cutting. *Procedia CIRP*, vol. 20, p. 98-102, **DOI:10.1016/j.procir.2014.05.037**.

[7] Zhang, Y.-L., Lei, J.-H. (2017). Prediction of laser cutting roughness in intelligent manufacturing mode based on ANFIS.

Procedia Engineering, vol. 174, p. 82-89, **DOI:10.1016/j.proeng.2017.01.152**.

[8] Zhang, K., Guo, X., Sun, L., Meng, X., Xing, Y. (2019). Fabrication of coated tool with femtosecond laser pretreatment and its cutting performance in dry machining SLM-produced stainless steel. *Journal of Manufacturing Processes*, vol. 42, p. 28-40, **DOI:10.1016/j.jmapro.2019.04.009**.

[9] Wang, T., Li, Y., Liu, J.,Qin, L., Wang, N., Zhang, L., Wang, H., Ll, Z. (2019). Milling force and surface topography of Ti-6Al-4V titanium alloy cladded by the laser. *Surface Review and Letters*, vol. 26, no. 5, art ID 1850185, **DOI:10.1142/S0218625X18501858**.

[10] Yi, J.H., Kang, J.W., Wang, T.J., Wang, X., Hu, Y.Y., Feng, T., Wu, P.Y. (2019). Effect of laser energy density on the microstructure, mechanical properties, and deformation of Inconel 718 samples fabricated by selective laser melting. *Journal of Alloys and Compounds*, vol. 786, p. 481-488, **DOI:10.1016/j.jallcom.2019.01.377**.

[11] Hatala, M., Duplák, J., Dupláková, D., Botki, F. (2019). Effect of traverse speed on surface roughness parameters after laser cutting of non-alloy structural steel. *Technology Education Management Informatics Journal*, vol. 8, no. 2, p. 402-408, **DOI:10.18421/TEM82-12**.

[12] Kim, D., Lee, S., Park, B. H., Kang, S. (2019). Analysis of the effects of supersonic assist gas for laser cutting using normal shock theory. *Transactions of the Korean Society of Mechanical Engineers B*, vol. 43, no. 4, p. 231-239, **DOI:10.3795/KSME-B.2019.43.4.231**.

[13] Feng, Y., Hung, T.-P., Lu, Y.-T., Lin, Y.-F., Hsu, F.-C., Lin, C.-F., Lu, Y.-C., Lu, X., Liang., S.Y. (2019). Surface roughness modeling in laser-assisted end milling of Inconel 718. *Machining Science and Technology*, vol. 23, no. 4, p. 650-668, **DOI:10.1080/10910344.2019.1575407**.

[14] Masoudi, S., Mirabdolahi, M., Dayyani, M., Jafarian, F., Vafadar, A., Dorali, R.M. (2019). Development of an intelligent model to optimize heat-affected zone, kerf, and roughness in 309 stainless steel plasma cutting by using experimental results. *Materials and Manufacturing Processes*, vol. 34, no. 3, p. 345-356, **DOI:10.1080/10426914.2018.1532579**.

[15] Dragu, D., Popescu, I., Sturzu, A. (1980). *Tolerances and Technical Measurements*, Didactica and Pedagogica Publishing House Bucharest. (in Romanian)

[16] Meško, J., Zrak, A., Nigrovič, R., Nikolić, R. R. (2018). The effect of selected technological parameters of laser cutting on the cut surface roughness. *Tehnički vjesnik - Technical Gazette*, vol. 25, no. 4, p. 997-1003, **DOI:10.17559/TV-20160609171348**.

[17] Rao, V.K., Murthy, P.B.G.S.N. (2018). Modeling and optimization of tool vibration and surface roughness in boring of steel using RSM, ANN and SVM. *Journal of Intelligent Manufacturing*, vol. 29, no. 7, 1533-1543, **DOI:10.1007/s10845-016-1197-y**.

[18] Adarsha Kumar, K., Ratnam, C., Venkata, Rao, K., Murthy, B.S.N. (2019). Experimental studies of machining parameters on surface roughness, flank wear, cutting forces and work piece vibration in boring of AISI 4340 steels: modelling and optimization approach. *SN Applied Sciences*, vol. 1, art ID 26, **DOI:10.1007/s42452-018-0026-7**.

[19] Riveiro, A., Quintero, F., Boutinguiza, M., del Val, J.,Comesana, R., Lusquinos, F., Pou, J. (2019). Laser cutting: A review on the influence of assist gas. *Materials*, vol. 12, no. 1, art. ID 157, **DOI:10.3390/ma12010157**.

[20] Spena, P.R. (2017). CO_2 laser cutting of hot stamping boron steel sheets. *Metals*, vol. 7, no. 11, art ID 456, **DOI:10.3390/met7110456**.

[21] Hirano, K., Fabbro, R. (2012). Possible explanations for different surface quality in laser cutting with 1 and 10 μm beams. *Journal of Laser Applications*, vol. 24, art ID 012006, **DOI:10.2351/1.3672477**.

[22] Zlámal, T., Malotová, S., Petru, J., Brytan, Z., Musil, V. (2018). The evaluation of the surface quality after laser cutting. *Innovative Technologies in Engineering Production*, vol. 244, art ID 02009, **DOI:10.1051/matecconf/201824402009**.

[23] Lazov, L., Nikolic, V, Jovic, S., Milovancevic, M., Deneva, H., Teirumenieka, E., Arsic, N. (2018). Evaluation of laser cutting process with auxiliary gas pressure by soft computing approach. *Infrared Physics & Technology*, vol. 91, p. 137-141, **DOI:10.1016/j.infrared.2018.04.007**.

[24] Wardhana, B.S., Anam, K., Ogana, R.M., Kurniawan, A. (2019). Laser cutting parameters effect on 316L stainless steel surface. *IOP Conference Series: Materials Science and Engineering*, vol. 494, art ID 012041, **DOI:10.1088/1757-899X/494/1/012041**.

[25] Sharifi, M., Akbari, M. (2019). Experimental investigation of the effect of process parameters on cutting region temperature and cutting edge quality in laser cutting of AL6061T6 alloy. *Optik*, vol. 184, p. 457-463, **DOI:10.1016/j.ijleo.2019.04.105**.